Mechanical Properties of Thermoplastic Waxy Maize Starch

J. J. G. VAN SOEST,[1,2,]* D. DE WIT,[1] and J. F. G. VLIEGENTHART[2]

[1]ATO-DLO, P.O. Box 17, 6700 AA Wageningen, and [2]Department of Bio-organic Chemistry, Bijvoet Center, Utrecht University, P.O. Box 80.075, 3508 TB Utrecht, The Netherlands

SYNOPSIS

The properties of thermoplastic amylopectin materials were investigated by stress–strain and relaxation measurements as a function of water content and crystallinity. Granular waxy maize starch was plasticized by extrusion with water and glycerol. The materials are amorphous after processing. The sharp fall in modulus at a water content of 10% is characteristic of a glass to rubber transition of an amorphous polymer. The materials are brittle below their glass transition temperature with a modulus of approximately 1000 MPa and an elongation of less than 20%. The amorphous rubbery materials are soft and weak with moduli of 0–10 MPa and tensile strengths of 0–2 MPa. The materials are viscoelastic, show plastic flow, and form a highly entangled polymer matrix, resulting in high values of elongation (500%), due to the high amylopectin molecular mass. Above glass transition temperature the amylopectin forms inter- and intramolecular double helices, crystallizing in a B-type crystal. The initial increase in modulus, tensile strength, and relaxation time is the result of the lower mobility of the amylopectin molecules and the reinforcement of the network by physical crosslinking. The drastic reduction of the elongation and the formation of cracks is the result of intramolecular crystallization. At crystalline junction zones the internal stress is increased and the interaction between molecules is reduced. © 1996 John Wiley & Sons, Inc.

INTRODUCTION

Recently, thermoplastic starch (TPS) products were developed solely on the basis of starch and natural additives such as water, glycerol, and lecithin.[1-7] These materials are totally biodegradable[8] and contribute to a reduction of the amount of plastic waste. The choice of a starch source is an important factor in regulating the properties of the TPS materials. The naturally occurring granular starches differ mainly in amylose and amylopectin content[9,10] as well as the molecular mass distribution and the degree of branching of both molecules.[11-13] No data are available on the mechanical properties of pure amylopectin TPS materials.

The properties of high and intermediate moisture materials, such as gels, cakes, and bread, are mainly determined by gelation, that is, the formation of an amylose and amylopectin network,[14-20] retrogradation, and crystallization.[21-23] During film casting starch retrogradation and crystallization is influenced by processing and storage conditions, such as drying temperature and time, and by composition, such as starch source and lipid content.[24] The main difference between the preparation of gels, foods, and films or the processing of TPS materials is the amount of water or plasticizer during the gelatinization or melting of the granular starch. To obtain thermoplastic starch, starch is melted with the aid of relatively low amounts of plasticizers during par example extrusion, pressure molding, and injection molding. The water content is in most cases lower than 20% during processing. Part of the water is usually replaced by low amounts of glycerol. Differences in water and glycerol content and processing conditions, such as shearing and temperature, leads to differences in starch network formation and morphology of the materials. Several types of crystalline structures are formed in TPS. The abundance of the structures is determined by plasticizer content,

---

processing, and storage conditions.[25] The TPS materials are exposed at various humidities during storage and their use. This results in variations in water content and glass transition temperature.[26] The stress–strain behavior of TPS depends on plasticizer content.[27-30] Glycerol was already shown to influence the crystallization kinetics of amylopectin.[31] Differences in the morphology and starch network lead to differences in the aggregation and crystallization behavior of the amylose and amylopectin compared to high moisture materials and cast films. An increase in B-type crystallinity in thermoplastic potato starch was shown to give an increase in elastic modulus and tensile strength and a decrease in elongation. Spontaneous cracking of TPS materials due to internal stresses was explained by an increase in intramolecular crystallization of amylopectin (data not shown).

The purpose of this article was to gain insight into the role of amylopectin in the variations in properties of the TPS materials. Waxy maize starch, which is composed of pure amylopectin, was processed by extrusion with water and glycerol as plasticizers. The materials were stored at various humidities to obtain a large variety of TPS materials with differences in water content and crystallinity. The influence of water content on the formation of the starch network was investigated. The effects of water content and crystallinity were related to the changes in the mechanical properties of the TPS materials.

EXPERIMENTAL

Extrusion

Samples were prepared by extruding narrow sheets using a Haake Rheocord 90 system equipped with a laboratory-scale counterrotating twin screw extruder fitted with a slit die. The dimensions of the die were 25-mm width and 0.4-mm thickness. Waxy maize starch (WCN; Amioca from Cerestar Gruppo Ferruzi) was premixed with glycerol [starch : glycerol ratio 100 : 27 (w/w)]. Three mixtures, batches WCN1, WCN2 [starch : water : glycerol ratio 68.7 : 10.3 : 21.0 (w/w)], and WCN3 [starch : water : glycerol ratio 69.4 : 9.6 : 21.0 (w/w)], were manually fed into the extruder. The torque varied between 30 and 65 N m for the batches with averages of batches 1, 2, and 3 of 45, 38, and 50, respectively. The screw rotation speed was 55 rpm. The temperature profile along the extruder barrel was 85, 140–145, 120, and 80–95°C (from feed zone to die). The melt temperature in zone 2 was 140°C. The slit die melt temperature was kept below 95°C to prevent the melt from boiling and to obtain a bubble-free extrudate. The thickness of the TPS materials was varied by variation in die temperature and by stretching the sheets with a calandar (Haake three-roll takeoff postex).

Conditioning

Part of the material was stored at −22°C after quenching in liquid nitrogen directly after extrusion. The rest was stored at relative humidities (RHs) between 0 and 100% at 20°C. After various time spans under these conditions, the materials were stored at 62 ± 4% RH and 20°C for 2 weeks after which mechanical testing and X-ray diffraction measurements were performed.

Moisture Analysis

Because of the tendency of TPS to adsorb or desorb water, special care was taken to measure the water content immediately at the time of testing. The samples were milled under cryogen conditions. The water content of the powder (1 g, size < 125 μm) was determined gravimetrically with a Gallenkamp vacuum oven operated at 70°C and a pressure of less than 100 mbar overnight. In view of the volatility of glycerol, the measurements did not exceed 24 h to minimize the loss of glycerol.

Mechanical Properties

A model 4301 Instron Universal Testing Machine operated at a grip length of 80 mm and crosshead speeds in the range of 1–500 mm/min was used for tensile and stress relaxation measurements. Dumbbell specimens, according to the ISO 1184-1983 (E) standard, were cut from the extruded ribbons directly after extrusion and stored. The sheet thickness varied and sample dimensions were corrected individually for the differences in initial thickness. Two to eight bars were measured and averaged for each series. The tensile stress at maximal load was calculated on the basis of the original cross-sectional area of the test specimen by the equation $\sigma = F/A$, wherein σ is the tensile stress, F is the force, and A is the initial cross-sectional area. The percentage strain or elongation was calculated on the basis of the length of the narrow parallel portion by the formula $(l - l_1)/l_1 \times 100\%$, where l is the distance be-
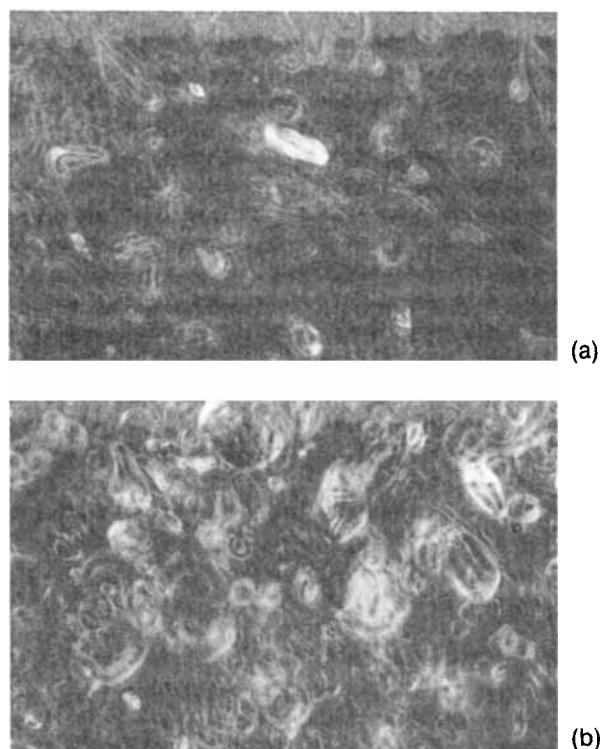
Figure 1 Polarized light microscopy of waxy maize starch TPS materials (batch WCN1) (a, 9.6% water) directly and (b, 13% water) after storage at 60% RH.

tween the gauge marks (in mm) and l_1 is length of the narrow parallel portion (i.e., 33 mm), which is related to the original gauge length, l_0 by $l_0/l_1 = 25/33$. The elastic modulus (E modulus) was calculated from the initial slope of the stress–strain curve. The energy to breakpoint, that is, tearing energy (J/mm^2), was calculated by the area under the stress–strain curve normalized by dividing through the area of the transverse section of the samples.

Stress relaxation measurements were done by pulling the materials at various crosshead speeds until the stress in the materials was on the order of 0–50% of the stress at the breakpoint obtained from the stress–strain curves at various crosshead speeds. The strain was kept constant and the change in stress was measured. The relaxation time, t, was defined as the time needed to give a decrease in stress of 30% measured from the initial load.

Differential Scanning Calorimetry (DSC)

DSC measurements were performed with a Perkin–Elmer DSC-7. Calibration was done with indium

(ΔH_{fusion} = 28.59 J/g, melting point (T_{onset}) = 156.60°C) and gallium (ΔH_{fusion} = 79.91 J/g, melting point (T_{onset}) = 29.78°C). An empty pan was used as a reference. Samples were weighed accurately into stainless steel pans and sealed hermetically. The glass transition temperatures were determined by heating the samples (30–40 mg) from 20 to 150°C at a rate of 10°C/min, followed by cooling down to −50°C at a rate of 200°C/min, and rescanned at a rate of 20°C/min to 200°C.

Polarized Light Microscopy

The materials were sliced and viewed at a magnification of 40× with a Axioplan Universal Microscope with photographs taken using the MC100 camera accessory.
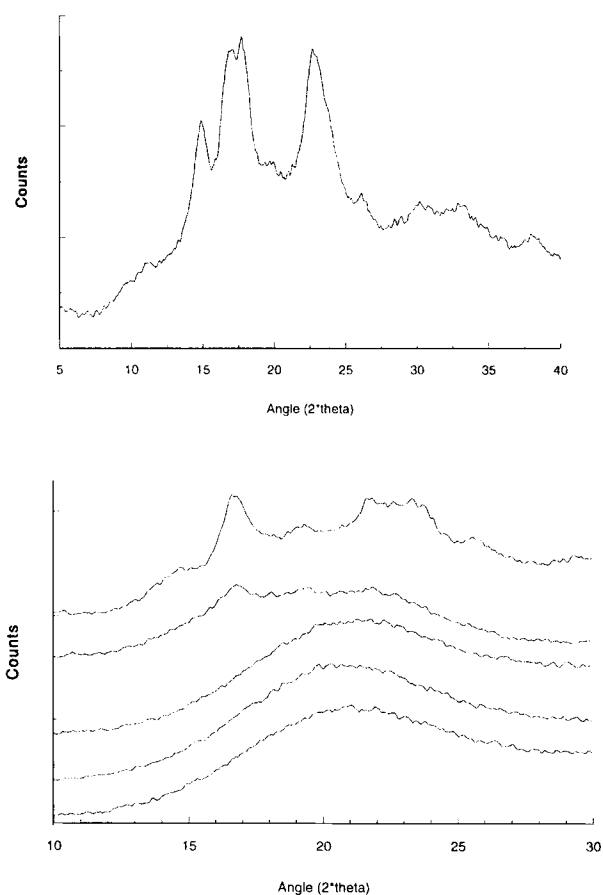

Figure 2 X-ray diffractograms of (top) granular waxy maize starch and (bottom) TPS materials of batch WCN1 stored at various temperatures and humidities. From bottom to top: quenched and stored for 2 weeks, stored at 40% RH for 2 weeks, stored at 60% RH for 2 weeks, stored at 70% RH for 8 months, and stored at 90% RH for 2 weeks.

**Table I   Glass Transition Temperatures at Various RH and Water Contents of Amorphous Materials**

Water %. (w/w)	RH (%)	$T_g \pm 5$ (°C)
20	75	ND
14	64	5
13	60	15
11	58	20
10	52	25
8	49	42
5	33	59

ND, not detectable.

X-Ray Diffractometry

Wide-angle X-ray diffractometry was performed with a Philips powder diffractometer (model PW 3710) operated at 2000 mW. The CuKα radiation, with a wavelength of 1.542 Å, was monochromized using a 15-μm Ni foil. The scattered radiation was detected using a proportional detector. Measurements of diffracted intensities were made in the angular range of 5-40° (°2θ) at ambient temperature. Crystallinity was measured according to the method of Hermans et al.[25] Diffractograms were smoothed (Savitsky-Golay, polynome = 2, points = 15) and the baseline corrected by drawing a straight line at an angle of 7°. The heights (H_c and H_t at 17.3°) and the areas (A_c and A_t between 16 and 18.5°) of the crystalline and total diffraction, respectively, were measured from the baseline. The ratios $R(X_H) = H_c/H_t$ and $R(X_A) = A_c/A_t$ are related to $\%X$ by the relations $\%X_{XRD} = (R(X_A) - 0.0090)/0.0040$ and $\%X_{XRD} = (R(X_H) - 0.095)/0.0055$. $\%X$ is defined as the relative crystallinity in comparison with native potato starch ($X_{XRD} = 1.0$ or $\%X_{XRD} = 100\%$). The crystallinity of native potato starch is approximately 25%. The relations were determined by measuring mixtures of amorphous and native potato starch in the range of 0-100%.
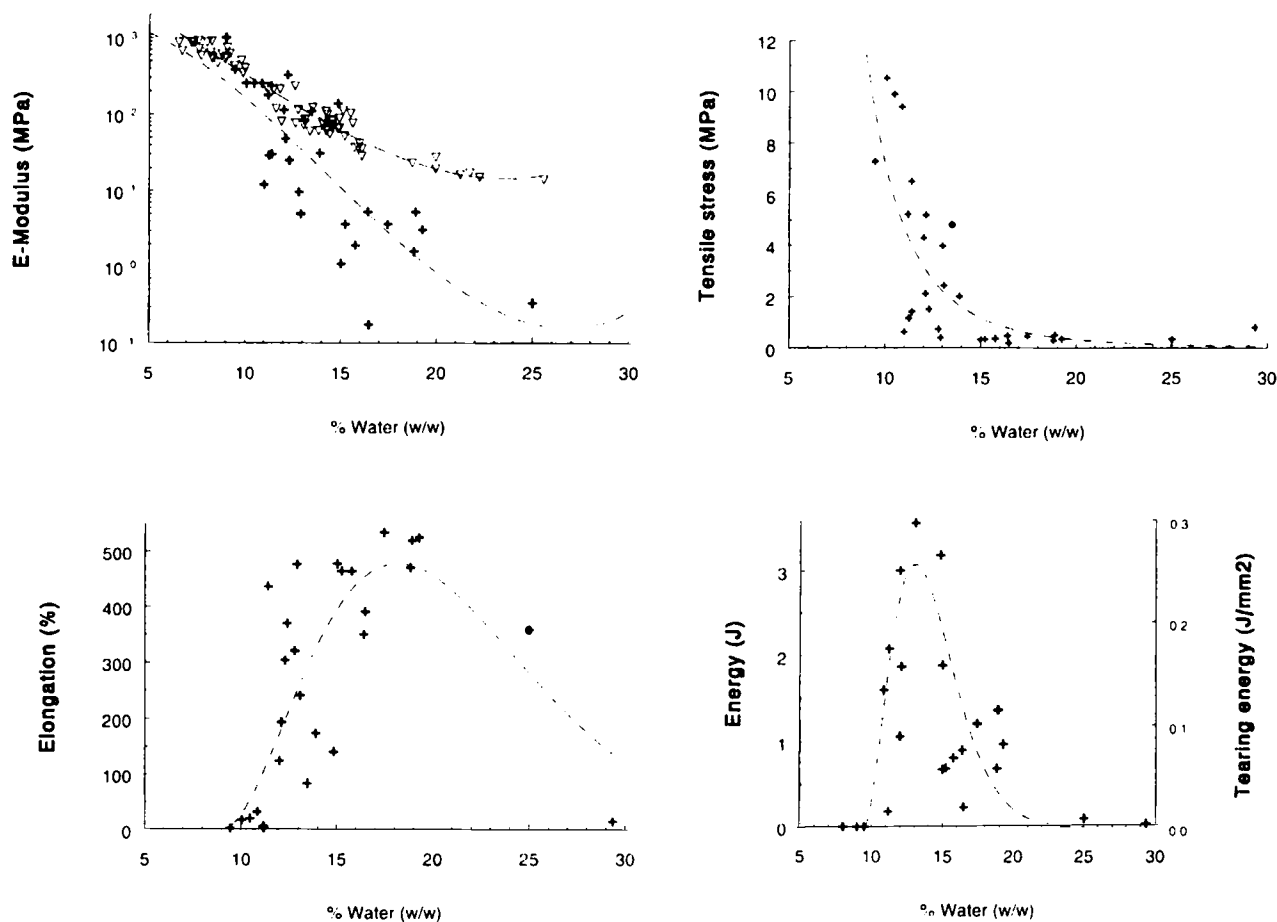
Figure 3   Mechanical properties of amorphous waxy maize TPS materials (batch WCN1) as a function of water content: (+) waxy corn starch, (∇) potato starch.
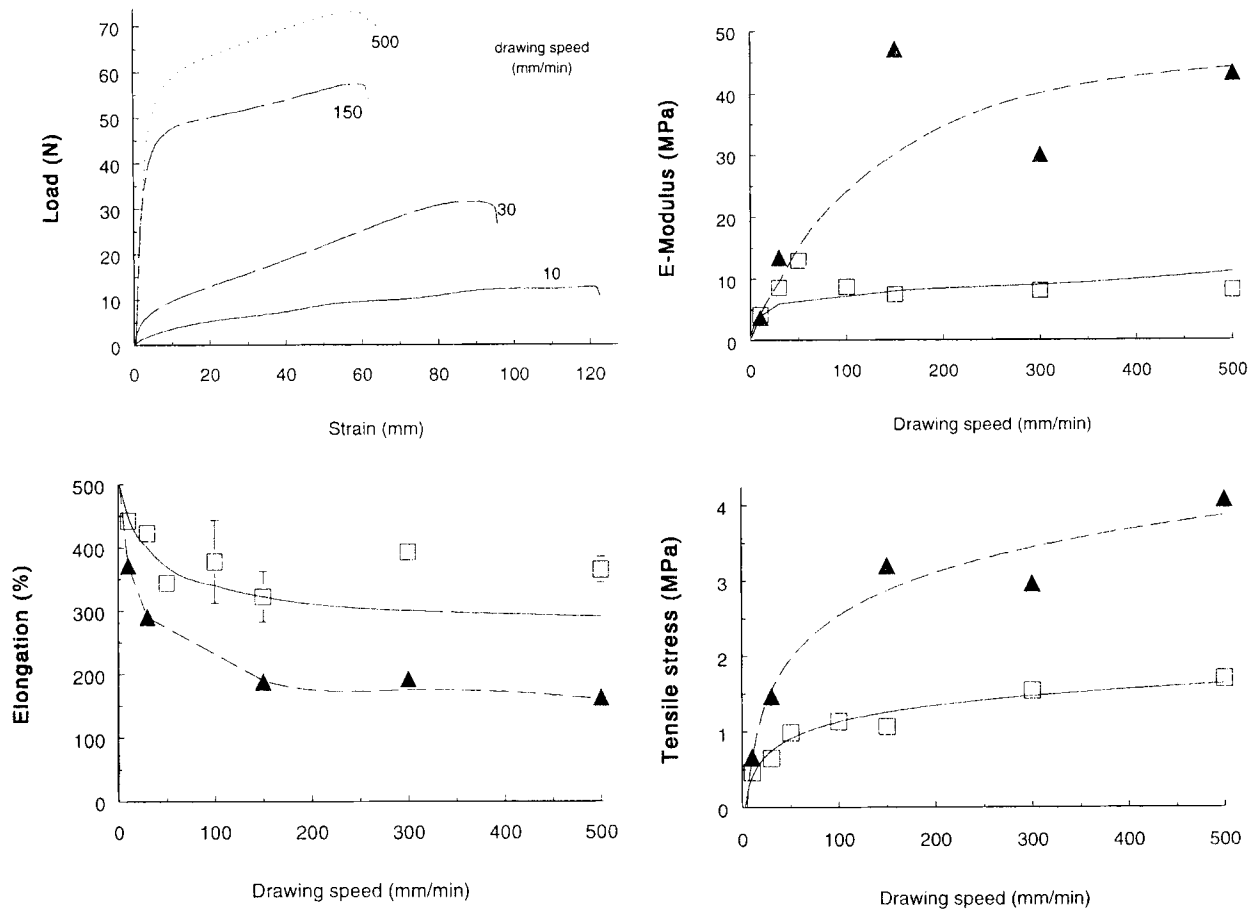
Figure 4   Load diagrams (upper left, 13–14% water) at different drawing speeds of amorphous TPS materials. Influence of drawing speed on the mechanical properties of amorphous TPS for two water contents (upper right and bottom): (□) 14–15% water, (▲) 13–14% water.

RESULTS AND DISCUSSION

Structural Characterization

Three different batches of TPS from waxy maize starch were obtained by extrusion. During extrusion the torque of batch WCN3 was somewhat higher than the torque of batches WCN1 and WCN2, suggesting a higher melting viscosity of the mixture with the lower water content. The TPS materials with a water content of 9.6% during extrusion (WCN3) were not flexible and broke easily directly after extrusion compared to the TPS materials with 10.3% water (WCN1 and WCN2). Extrudates of all samples were translucent, suggesting that the granular structure of the waxy maize starch was destroyed during extrusion. Due to the high shear and temperature conditions, almost all granules broke up

into small fragments, and no birefringence of intact granules was observed (Fig. 1).

Some typical X-ray diffractometer scans of the granular and the extruded waxy maize TPS materials, stored at various humidities, are shown in Figure 2. Granular waxy maize starch has the A-type structure, while the extruded materials are amorphous or have small amounts of the B-type crystallinity. It is apparent from these data that all the A-type crystallinity found in the native granule was melted during extrusion, resulting in completely amorphous TPS material. The measured processing melt temperature (140°C) was relatively low to obtain complete melting of the waxy maize granular crystallinity compared to the melt temperatures observed at low shearing conditions, such as during the DSC experiments (up to 170°C). However, it has to be noted that the melt temperature can be
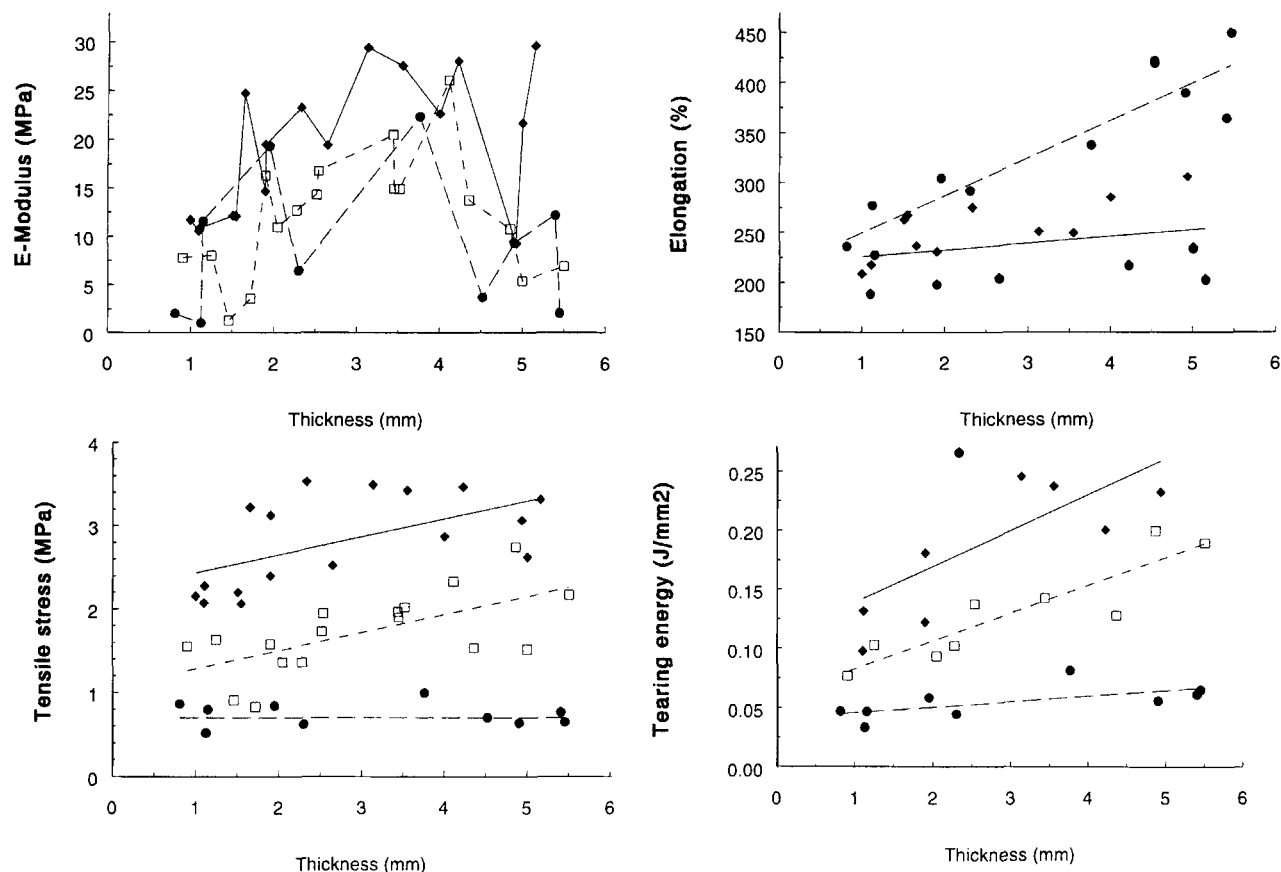
Figure 5 Influence of thickness of amorphous TPS materials (batch WCN3 with 14% water) on the determination of the stress–strain properties for various drawing speeds: (◆) 500 mm/min, (□) 150 mm/min, (●) 10 mm/min.

higher locally than the measured barrel temperatures because of the heat produced during mechanical shearing of the melt. Moreover, the breakdown of the granule due to shearing increased the availability of the plasticizers during processing, resulting in a lower melting temperature compared to the temperatures observed with the DSC experiments.

Materials with a water content of approximately 10% and a glass transition temperature of 25°C (as determined with DSC), which were stored below their glass transition temperature at −22°C, showed no crystallinity. In Table I the measured glass transition temperatures are shown at various water contents and RH of amorphous materials. For materials with a water content above 14%, which were stored at 20°C and RH above 50%, a B-type crystallinity was observed. The rate of crystallization was highly dependent on the RH and water content. At 90% RH the highest level of crystallinity of the starch in the waxy maize TPS materials was already obtained after about 2 weeks; during long-term storage

at 70% RH this level was still not reached. At 60% RH (TPS with less than 14% water) no crystallization was observed during the first 2 weeks. The highest level of crystallinity measured was approximately 18%. Apparently, the B-type crystallinity observed after storage of the materials was entirely due to recrystallization. The crystallization behavior of the amylopectin starch was regulated by the glass transition temperature of the TPS materials as a function of water content. Below the glass transition temperature the materials were glassy. This means that the molecular motion was low and that crystallization did not occur in a finite period of time.

Tensile Properties of Amorphous Materials

Some typical load–strain diagrams of amorphous materials at various water contents are shown in Figure 4 (upper left). The influence of water content on the stress–strain behavior of the TPS materials is shown in Figure 3. The plots are essentially linear
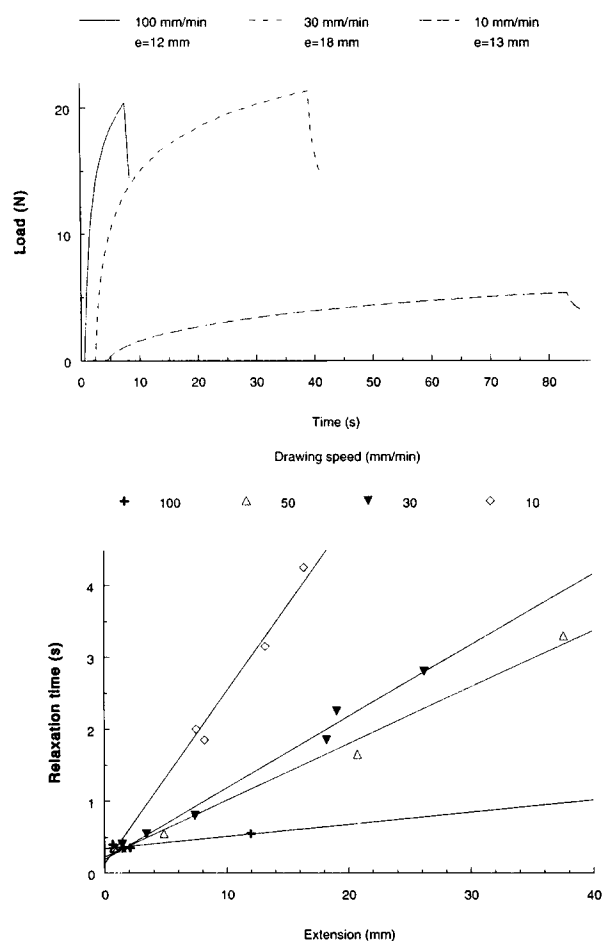
Figure 6 Stress–relaxation behavior of amorphous waxy maize TPS materials (batch WCN3 with 14% water) vs. (top) drawing speed and (bottom) extension (e).

at low strains and curve toward the strain axis at higher strains. At water contents less than 8% the materials were glassy and too brittle to be measured. A sharp decrease in E modulus and tensile stress and an increase in elongation was observed at a water content of 11–13%. The materials with a water content of 13–20% behave in a rubbery fashion. The change of brittle to ductile behavior with increasing plasticizer content was characteristic of a polymer being plasticized through its glass transition temperature. For potato starch and hydrolyzed potato starch TPS materials the change in behavior from brittle fracture to tearing, a slow fracturing process characteristic of the rubbery state, was not as pronounced as for these waxy maize starch materials.[30] The waxy maize starch materials were less complex in composition than the potato starch TPS materials, which are composed of a complex mixture of partially crystalline amylose and amylopectin. The

less complex nature of the waxy maize starch materials gave rise to a smaller range of glass transition temperatures.

Amorphous waxy maize TPS materials in the rubbery state are very weak and soft, having low tensile strengths and E moduli. The values are low compared to the observed values of semicrystalline thermoplastic starch materials composed of the amylose containing starches.[26–30] Rubbery amorphous materials can be stretched to very high ultimate elongations on the order of magnitude of 300–500%, even at water contents of 19–20%. The materials are weak because fracture occurs mainly between segments at different chains; thus, the fracture strength is low because only intermolecular bonds, such as Vanderwaals forces and H bridges, are severed. Several yield points were observed in the stress–strain curves. The observed necking, that is,
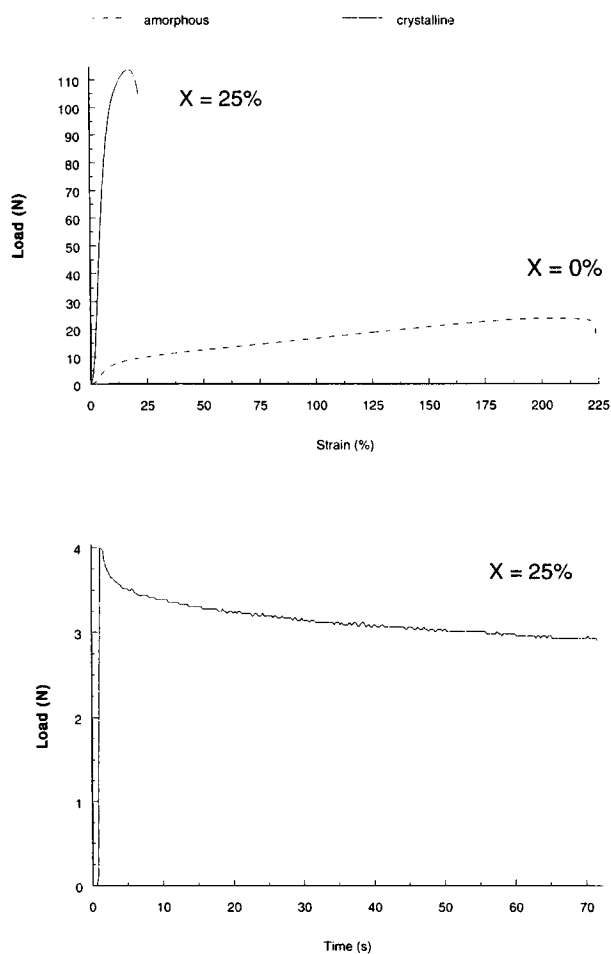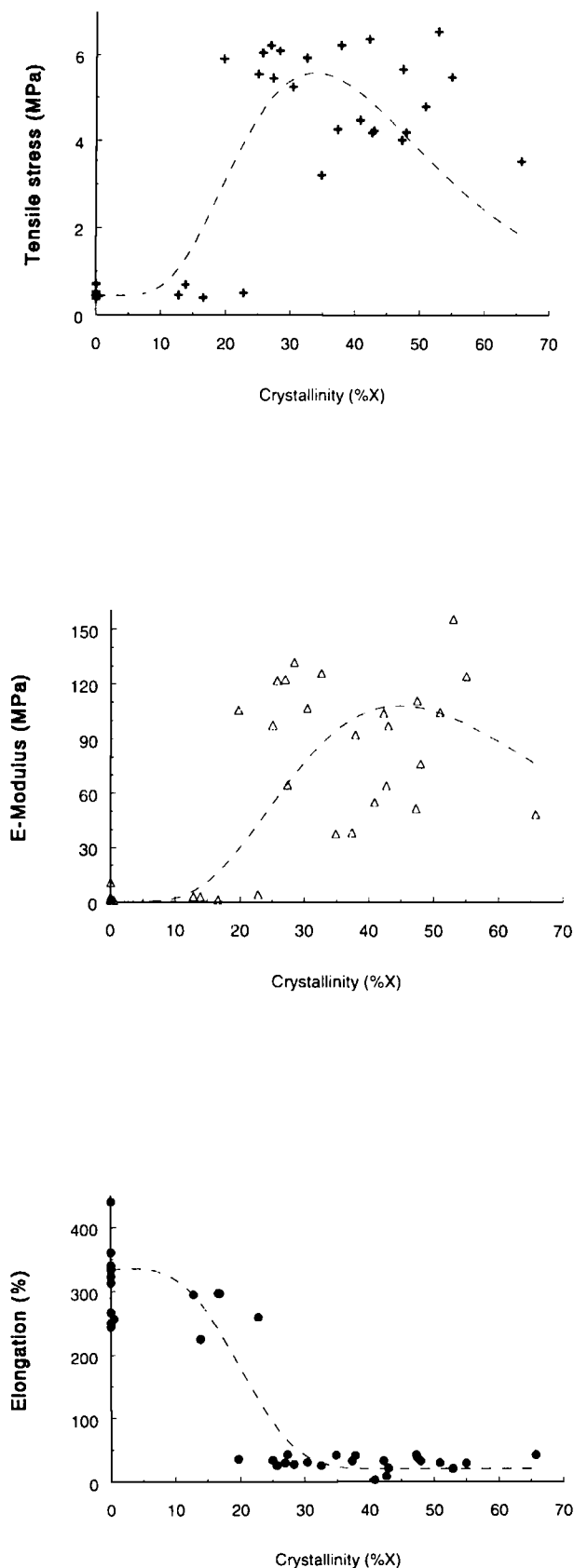

Figure 7 Influence crystallinity on the (top) load–strain and (bottom) load–relaxation behavior of waxy maize TPS materials with $X = 0$ and 25%, and 14% water.

Crystallinity (%X)

Crystallinity (%X)

Crystallinity (%X)

reduction of initial area of the tensile bar, and yielding in the materials due to stress softening and subsequent stress hardening seemed to be a multistep mechanism (telescope effect).

The effect of drawing speed on the stress–strain properties of amorphous materials tested at a water content of 14–15% and 13–14%, respectively, and as a function of material thickness are shown in Figures 4 and 5, respectively. The greater the drawing speed is, the steeper the load–strain curves, and the smaller the ultimate elongations [Fig. 4 (upper left)]. The materials with a water content of 13–14% had a lower glass transition temperature and showed, with increasing pulling rate, a relatively large effect on the E modulus, tensile strength, and elongation in comparison with materials with 14–15% water. However, the materials were weak, even at very high pulling rates, with elongations in the range of 150–500%. This polymer behavior is comparable to polyethylene terephthalate.[32] The amylopectin polymer had less time to flow at high pulling rates and the TPS material behaved more rigidly. The viscous or plastic flow was influenced by drawing speed because time has an effect on the slipping of the polymer chain segments past each other and the detangling of the entangled chain segments. The response of the amylopectin molecules was more elastic at higher drawing speeds. At high pulling rates the interactions between chains and entanglements behaved more like permanent crosslinkages, resulting in a decreased mobility and an increase in E modulus and fracture strength. The molecules were not able to slip and detangle completely. More bonds were broken and the strain at break decreased. The chain segments responsible for entanglements and intermolecular interactions, such as H bridges and double helical formations, were most likely the outer chains of the amylopectin molecules.[11-13] These chains were short with an average degree of polymerization below 20, which explains the low tensile stress even at high pulling rates.

The materials were very irregular in thickness (0.5–5.5 mm) due to extrudate swell (or die swell). This extrudate swell was relatively large and dependent on die temperature, throughput, and shear. Also the water content during extrusion and the water content directly after extrusion (RH of the laboratory) was of influence. Batch WCN3, which was ex-

Figure 8 Influence degree of crystallization on the stress–strain properties of the waxy maize TPS materials at a water content of 13–15%.

truded with less water than batches WCN1 and WCN2 (9.6 vs. 10.3% water), showed a relatively low amount of extrudate swell (0.5–3.0 mm). No significant change in modulus was observed with changes in thickness, although it must be taken into account that the materials were too weak to get accurate data of the E modulus. The elongation was independent of thickness at low drawing speeds but increased at higher drawing speeds. The stress at peak or break and the tearing energy showed the reversed effect and increased for thicker materials at high drawing speeds. At low drawing speeds the detanglement of the amylopectin resulted in a longer time to break the material over the entire area of the sample. As a result the elongation increased with an increase in thickness. The stress and the energy dissipated was therefore higher as a result of drawing speed, but no effect of thickness was expected because both were corrected as a first approximation for differences in initial thickness. Still a residual effect was observed as a function of thickness; the tearing energy increased with increasing initial thickness. The corrections were only made for differences in initial area and did not consider the correct true area and true length after an elongation, which led to deviations in measured nominal values and true values of the stress and tearing energy. The stretching of the rubbery materials during processing led to a decrease in thickness of the materials that resulted also in a decrease of the elongation at rupture, the stress at break, and the tearing energy. No discrimination between the effects of stretching and differences in nominal and true values could be made on the basis of the measurements.

Stress Relaxation of Amorphous Materials

For amorphous TPS materials the relaxation behavior was measured. Typical load–strain–relaxation behavior is shown in Figure 6. The materials show a permanent deformation after stress–strain measurements up to 40% of the initial length of the tensile bars. For materials with a water content above 15%, it was not possible to get reproducible results, because the materials were too weak to be measured accurately. The measurements shown are for rubbery materials of batch WCN2 stored at 55–60% RH with a water content of 13–14%. The relaxation time was increased with decreasing pulling rate and with increasing extension or strain. This behavior is typical for viscoelastic materials. The ratio of the relaxation times and the time scale of the experiments (Deborah number[33]) was on the or-

der of magnitude of 0–1, which is characteristic of a viscous polymer melt. At high drawing rates or at low extensions the response of the materials was completely elastic. The response can be described by a mechanical model of a spring for an elastic Hookean body. This spring is not able to relax. The viscous component of the TPS material needed time to respond and was unaffected at high speeds and low extensions, that is, no viscous deformation took place. The viscous part of the materials needed time to respond to the imposed strain. The stress relaxation was entirely due to the viscous part of the materials at constant extension. The relaxation time was low for materials with a large viscous component. At low pulling rates and high extensions the response of the materials was partly viscous and the relaxation of the materials took place over a longer time span.

Influence Aging and Crystallinity

Batches WCN1 and WCN2 were extruded with a higher amount of water (10.3%) than batch WCN3 (9.6%). This resulted in different behavior during storage above glass transition temperature. Batches WCN1 and WCN2 showed almost no change in length during storage above glass transition while batch WCN3 showed remarkably large changes in length, up to 50%. This relaxation of the material was accompanied by a change in flexibility of the materials. Highly flexible materials were not changed in length. The starch molecules in the materials of batch WCN3 were stretched during extrusion in the direction of the flow. This orientation was detained at low water contents and at temperatures below or close to the glass transition temperature. One could say that the extrudate swell was partly frozen in. During storage at higher water contents (70% RH) the stretched molecules attempted to attain a random coil conformation and the material shrunk. The increase in mobility resulted also in an increase in crystallinity.

Characteristic load–strain diagrams of an amorphous ($X = 0\%$) and a crystalline ($X = 25\%$) material at identical water contents are shown in Figure 7(top). The stress–strain curve of the amorphous material is characteristic of a soft and rubber-elastic material, while the crystalline materials are brittle. The results of the mechanical properties versus crystallinity for the various conditions are shown in Figure 8. It is clear that a sharp increase in E modulus and stress and a decrease in elongation was observed at a crystallinity of approximately 20%.

Also the amount of spontaneously broken materials was increased at high crystallinity. For most materials with a $\%X > 30\%$, mechanical testing was not possible because of the large amount of cracks. For the materials stored at 90% RH for more than 2 weeks, the relative crystallinity was in the range of 70–80%. These materials showed a large amount of cracks and broke spontaneously. The effect of crystallinity on the relaxation of the materials is shown in Figure 7(bottom) for a material with $X = 25\%$. The relaxation time increased drastically compared to an amorphous material. The changes in stress–strain and relaxation behavior were explained by an increase in the initial formation of double helical structures of the amylopectin outer chains. These helices can aggregate to form crystalline regions in the materials. This reduces the mobility of the amylopectin molecules resulting in an increase of the E modulus. The strength of the materials increased because the plastic flow of crystalline materials was reduced and more covalent bonds were severed. The formation of physical crosslinks also reduced the elongation. The formation of intermolecular double helices and crystalline regions reinforced the amylopectin matrix; but the formation of intramolecular crystals within one amylopectin molecule weakened the formed network by a reduction of the interaction between separate molecules, and the coherency within the material was lost. The formation of intramolecular crystalline regions was favored and led to internal stress within the materials. At the junction zones between two crystalline amylopectin molecules the molecular interactions were lost, and the material formed cracks, reducing the strength and the elongation.

CONCLUSIONS

Polymer principles developed for synthetic polymers were successfully applied to describe the properties of TPS materials. During extrusion processing of granular waxy maize starch a thermoplastic material was obtained. The amylopectin molecules were highly oriented during extrusion processing. The waxy maize TPS materials were viscoelastic with a glass to rubber transition dependent on water content. The high elongation and the flexibility of the amorphous materials was due to the combination of the high molecular mass of the amylopectin molecules and the easy slipping of the amylopectin molecules along each other, that is, plastic flow.

Above glass transition temperature or at high water contents, the amylopectin formed inter- and intramolecular double helices. Aggregation of double helices led to B-type crystallinity. Intermolecular crystallinity led to a reinforcement of the network by the formation of physical crosslinks. Intramolecular crystallization of the amylopectin lowered the mobility of the amylopectin and increased the stress in the material at highly crystalline junction zones. The mechanical properties were characteristic of partially crystalline polymers. At crystalline regions, the TPS materials broke spontaneously. Thus, in starch plastics the problem of the decline in material properties in time is at least partly due to the reorganization and crystallization of the amylopectin molecules.

REFERENCES

1. L. S. Lay, J. Rehm, R. F. T. Stepto, M. Thoma, J. P. Sachetto, D. J. Lentz, and J. Silbiger, U.S. Pat. 5,095,054 (1992).
2. C. Bastioli, V. Bellotti, L. Del Giudice, and R. Lombi, Italy Pat. Int. Appl. WO 9,102,025 (1991).
3. R. F. T. Stepto, I. Tomka, and M. Thoma, Eur. Pat. Appl. EP 304,401 (1989).
4. H. Röper and H. Koch, *Starch/Stärke*, **42**, 123 (1990).
5. W. Wiedmann and E. Strobel, *Starch/Stärke*, **43**, 138 (1991).
6. C. Bastioli, V. Bellotti, G. Del Tredici, R. Lombi, A. Montino, and R. Ponti, Italy Pat. Int. Appl. WO 9,219,680 (1992).
7. I. L. H. A. De Brock, P. M. R. Van den Broecke, and K.-H. Bahr, Eur. Pat. Appl. EP 599,535 (1993).
8. M. Van der Zee, L. Sijtsma, G. B. Tan, H. Tournois, and D. de Wit, *Chemosphere*, **28**, 1757 (1994).
9. M. Kugimiya and J. W. Donovan, *J. Food Sci.*, **46**, 765 (1981).
10. D. Sievert and J. Holm, *Starch/Stärke*, **45**, 136 (1993).
11. S. Hizukuri, *Carbohydr. Res.*, **147**, 342 (1986).
12. S. Hizukuri and T. Tagaki, *Carbohydr. Res.*, **134**, 134 (1984).
13. C. Takeda, Y. Takeda, and S. Hizukuri, *Carbohydr. Res.*, **246**, 273 (1993).
14. K. Svegmark, S. Kidman, and A.-M. Hermansson, *Carbohydr. Polym.*, **22**, 19 (1993).

15. V. M. LeLoup, P. Colonna, and A. Buleon, *J. Cereal Sci.*, **13**, 1 (1991).
16. M. L. German, A. L. Blumenfeld, Y. V. Guenin, V. P. Yuryev, and V. B. Tolstoguzov, *Carbohydr. Polym.*, **18**, 27 (1992).
17. M. J. Miles, V. J. Morris, P. D. Orford, and S. G. Ring, *Carbohydr. Res.*, **135**, 271 (1985).
18. P. D. Orford, S. G. Ring, V. Carroll, M. J. Miles, and V. J. Morris, *J. Sci. Food Agric.*, **39**, 169 (1987).
19. S. G. Ring, P. Colonna, K. J. l'Anson, M. T. Kalichevsky, M. J. Miles, V. J. Morris, and P. D. Orford, *Carbohydr. Res.*, **162**, 277 (1987).
20. P. L. Russell, *J. Cereal Sci.*, **6**, 147 (1987).
21. A.-C. Eliasson and L. Bohlin, *Starch/Stärke*, **34**, 267 (1982).
22. B. J. Bulkin, Y. Kwak, and I. C. M. Dea, *Carbohydr. Res.*, **160**, 95 (1987).
23. C. G. Biliaderis and J. Zawistowski, *Cereal Chem.*, **67**, 240 (1990).
24. H. G. Bader and D. Göritz, *Starch/Stärke*, **46**, 435 (1994).
25. J. J. G. van Soest, S. H. D. Hulleman, D. de Wit, and J. F. G. Vliegenthart, *Ind. Crops Prod.*, **5**, 11 (1996).
26. M. T. Kalichevsky, E. M. Jaroszkiewicz, and J. M. V. Blanshard, *Polymer*, **34**, 346 (1993).
27. A. R. Kirby, S. A. Clark, R. Parker, and A. C. Smith, *J. Mater. Sci.*, **28**, 5937 (1993).
28. A.-L. Ollett, R. Parker, and A. C. Smith, *J. Mater. Sci.*, **26**, 1351 (1991).
29. P. A. Dell and W. G. Kohlman, *J. Appl. Polym. Sci.*, **52**, 353 (1994).
30. J. J. G. van Soest, K. Benes, D. de Wit, and J. F. G. Vliegenthart, *Polymer*, to appear.
31. J. J. G. van Soest, H. Tournois, D. de Wit, and J. F. G. Vliegenthart, *Polymer*, **35**, 4721 (1994).
32. M. Beyer and E. Schollmeyer, *Angew. Makromol. Chem.*, **60/61**, 53 (1989).
33. H.-G. Elias, *An Introduction to Plastics*, VCH, Weinheim, Germany, 1993.